BEILSTEIN JOURNAL OF ORGANIC CHEMISTRY

Interaction of a pyrene derivative with cationic [60]fullerene in phospholipid membranes and its effects on photodynamic actions

Hayato Takagi[1], Çetin Çelik[2], Ryosuke Fukuda[1], Qi Guo[3], Tomohiro Higashino[3], Hiroshi Imahori[3,4,5], Yoko Yamakoshi[2] and Tatsuya Murakami[*1,4]

Letter

Open Access

Address:
[1]Department of Biotechnology and Pharmaceutical Engineering, Graduate School of Engineering, Toyama Prefectural University, 5180 Kurokawa, Imizu City, Toyama 939-0398, Japan, [2]Laboratorium für Anorganische Chemie, ETH Zürich, CH-8093 Zürich, Switzerland, [3]Department of Molecular Engineering, Graduate School of Engineering, Kyoto University, Nishikyo-ku, Kyoto 615-8510, Japan, [4]Instutite for Integrated Cell–Material Sciences (iCeMS), Kyoto University, Sakyo-ku, Kyoto 606-8501, Japan and [5]Instutite for Liberal Arts and Sciences (ILAS), Kyoto University, Sakyo-ku, Kyoto 606-8501, Japan

Email:
Tatsuya Murakami* - murakami@pu-toyama.ac.jp

* Corresponding author

Keywords:
liposome; π–π interaction; reactive oxygen species; superoxide radical anion

Beilstein J. Org. Chem. **2024,** *20,* 2732–2738.
https://doi.org/10.3762/bjoc.20.231

Received: 12 July 2024
Accepted: 01 October 2024
Published: 30 October 2024

This article is part of the thematic issue "Carbon-rich materials: from polyaromatic molecules to fullerenes and other carbon allotropes".

Associate Editor: C. Stephenson

Abstract

We have reported that upon visible light irradiation, ferrocene-porphyrin-[60]fullerene triad molecules yield long-lived charge-separated states, enabling the control of the plasma membrane potential (V_m) in living cells. These previous studies indicated that the localization of the triad molecules in a specific intra-membrane orientation and the suppression of the photodynamic actions of the [60]fullerene (C_{60}) moiety are likely important to achieve fast and safe control of V_m, respectively. In this study, by mimicking our previous system of triad molecules and living cells, we report a simplified model system with a cationic C_{60} derivative ($catC_{60}$) and a liposome with embedded 1-pyrenebutyric acid (PyBA) to demonstrate that the addition of PyBA was important to achieve fast and safer control of V_m.

Introduction

The [60]fullerene (C_{60}) is known as an excellent electron acceptor [1,2] and is commonly used in organic solar cell applications [3]. Taking advantage of the fact that C_{60} can be an acceptor in photoinduced charge-separation systems, we have previously employed ferrocene-porphyrin-C_{60} triad molecules (Figure 1a) in a biological system to control the plasma mem-

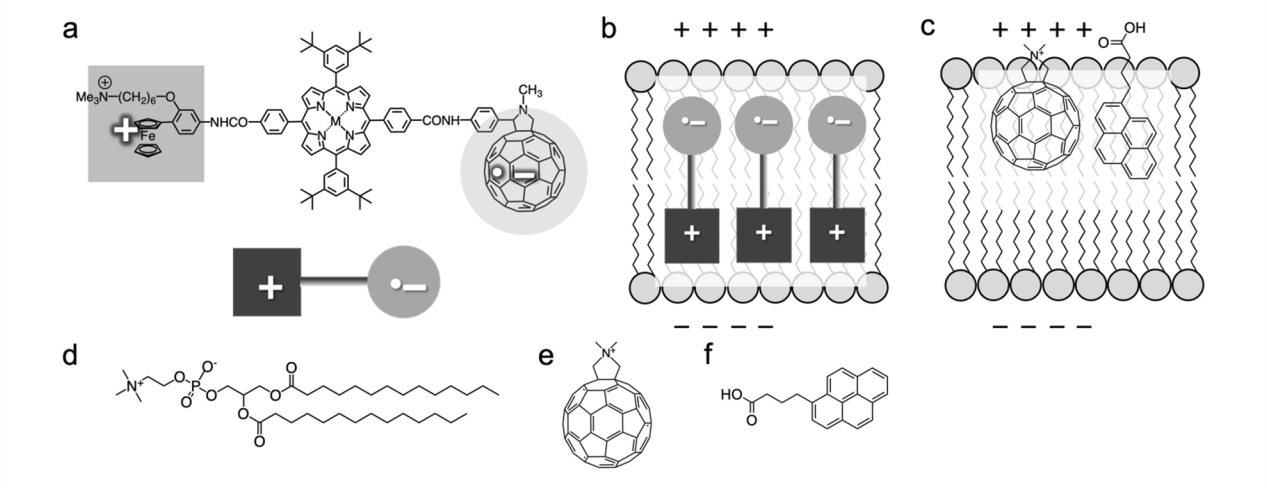

Figure 1: (a) Chemical structure and schematic illustration of the charge-separated state of a triad molecule and (b) control of the membrane potential by the illuminated molecule with a favourable arrangement. (c) Strategy of the present study for controlling both the location and photodynamic actions of a cationic derivative of C_{60} ($catC_{60}$), a simple model compound of the triad molecules, in a membrane via π–π interactions with 1-pyrenebutyric acid (PyBA). (d–f) Chemical structures of 1,2-dimyristoyl-*sn*-glycero-3-phosphocholine (DMPC) (d), $catC_{60}$ (e), and PyBA (f).

brane potential (V_m) of living mammalian neuronal cells under photoirradiation [4-6]. Generally, V_m originates from a difference in electric charge on the two sides of the plasma membrane (approximately 5 nm thickness), with a slight excess of the positive ions inside relative to the negative ions outside. Our ferrocene-porphyrin-C_{60} triad molecule exhibited long-lived charge-separated states under visible light irradiation [7], with the C_{60} species becoming negatively charged while the ferrocene moiety became positively charged (Figure 1a). This charge-separated state can be used to initiate nanoscale electric fields, e.g., V_m. The design of the triad molecules may also help to keep their orientation within the plasma membrane to have the C_{60} moiety located near the outer membrane surface and the ferrocene moiety near the inner membrane surface (Figure 1b). With this favorable arrangement of the molecules, it was expected to trigger a photoinduced change of the V_m that occurs at very fast time scales (less than milliseconds), leading to the (partial) cancellation of the V_m. However, in reality, the change occurred on a minute time scale, indicating that the favorable arrangement was not sufficiently achieved in the plasma membrane.

One of the concerns with our previous triad molecules was photoinduced generation of reactive oxygen species (ROS) [8]. In our more recent study, the reversal of V_m after stopping photoirradiation of our triad molecule was associated with the renewal of the plasma membrane through endocytosis in living cells [6]. These results suggested that the photoinduced change in V_m was caused by some modification – most likely oxidation – of the plasma membrane by the photoexcited triad molecule. Taken together, for the realization of rapid control of V_m using such C_{60}-based molecules in the membrane, the suppression of ROS generation is an important consideration. In this study, we aim to develop a system to achieve a quick V_m control without damaging the membranes by using a C_{60} derivative and a pyrene derivative as a model system for the triad molecules.

C_{60} has been reported to be incorporated into the phospholipid bilayers at the central part of membrane due to its hydrophobicity [9,10]. In contrast, to achieve the favorable arrangement as described above, the C_{60} moiety of the triad molecule needs to be located near the outer membrane surface. To facilitate this arrangement, in this study, we utilized a simplified system (Figure 1c) consisting of (i) liposomes of 1,2-dimyristoyl-*sn*-glyreco-3-phosphocholine (DMPC, Figure 1d), a well-known model of the plasma membrane, (ii) a cationic derivative of C_{60} ($catC_{60}$, Figure 1e) as a replacement of the triad molecules, and (iii) 1-pyrenebutyric acid (PyBA, Figure 1f) as an anchor molecule for $catC_{60}$ to be localized near the surface of phospholipid membranes [11,12]. With this model system, we aimed to examine whether both the intramembrane localization and the photodynamic actions of $catC_{60}$ can be modulated by PyBA.

Results and Discussion

The $catC_{60}$-loaded liposomes ($catC_{60}$-lip) were prepared by hydration of a $catC_{60}$-embedded DMPC film [13] and compared with C_{60}-loaded liposomes (C_{60}-lip) by physicochemical characterizations. When $catC_{60}$ or C_{60} was added to DMPC (in a 1:1 molar ratio to DMPC) the zeta potential of the $catC_{60}$-lip was higher (16 mV) than that of C_{60}-lip (–0.3 mV). Based on the experiments of differential scanning calorimetry analyses with varied amount of $catC_{60}$ or C_{60} (Figure 2a), the addition of $catC_{60}$ caused the disappearance of phase transition of DMPC liposomes in a dose-dependent manner and more efficiently

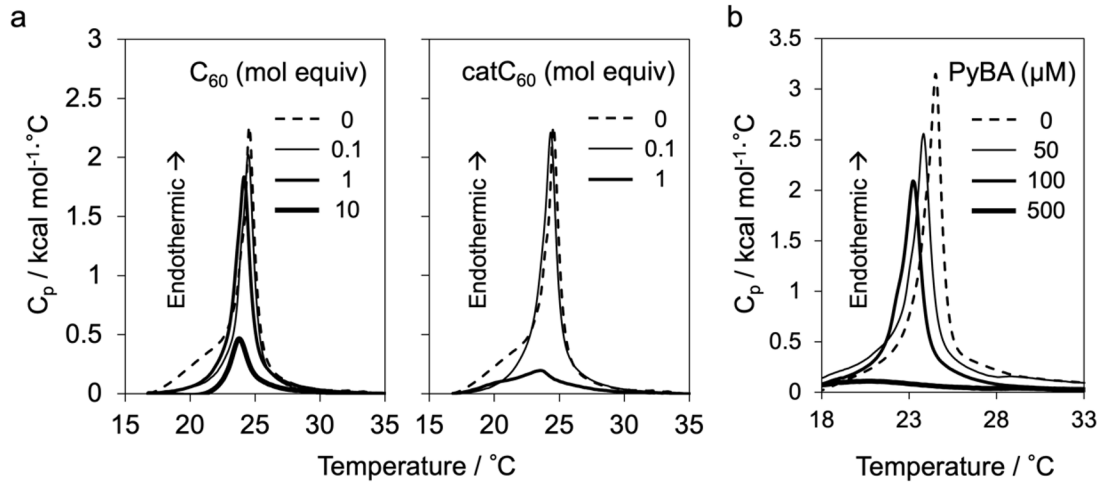

Figure 2: Differential scanning calorimetry analysis for the phase transition of liposomes (1 mM phospholipid). (a) Effect of the addition of C_{60} (left) or a cationic derivative of C_{60} ($catC_{60}$) (right) at various molar equivalents (mol equiv) to the phospholipid of liposomes. (b) Effect of 1-pyrenebutyric acid (PyBA) addition at various concentrations to liposomes without $catC_{60}$ and C_{60}. The gel-to-liquid crystalline phase transition for 1,2-dimyristoyl-*sn*-glycero-3-phosphocholine (DMPC) liposomes was observed at 25 °C. All the measurements were performed with liposome samples dispersed in phosphate-buffered saline (PBS(–)).

than the case with C_{60}. These results suggested that $catC_{60}$ was more likely to localize near the surface of the lipid bilayer of $catC_{60}$-lip than the C_{60} in C_{60}-lip [14]. Similarly, the incorporation of PyBA into the pre-prepared liposomes was tested by zeta potential analysis (–15 mV) and differential scanning calorimetry analysis (Figure 2b), showing a clear dose dependency on the amount of PyBA added.

The absorption spectra of $catC_{60}$-lip and C_{60}-lip were compared in PBS(–) (Figure 3). At two different concentrations, no significant change was observed in $catC_{60}$-lip, whereas broadening and a red shift were observed in C_{60}-lip at higher concentrations (10 mol equiv). These results indicate that $catC_{60}$ was better dispersed in the DMPC membrane than C_{60}. The results also provided some insight into the situation of our previous triad molecule – how the undesired aggregate formation of the triad molecules is reduced during solubilization and cell studies in physiologically relevant media [15].

The interaction between $catC_{60}$ and PyBA in the liposomes was assessed by the fluorescence spectra of PyBA in $catC_{60}$-lip [16]. The $catC_{60}$-lip containing $catC_{60}$ at 0, 5.4, and 54 μM were mixed with PyBA (50 μM) in PBS(–), and the fluorescence spectra were measured. As shown in Figure 4a, the intensity decreased upon increasing the concentration of the $catC_{60}$ in the liposomes, showing the quench of PyBA fluorescence by

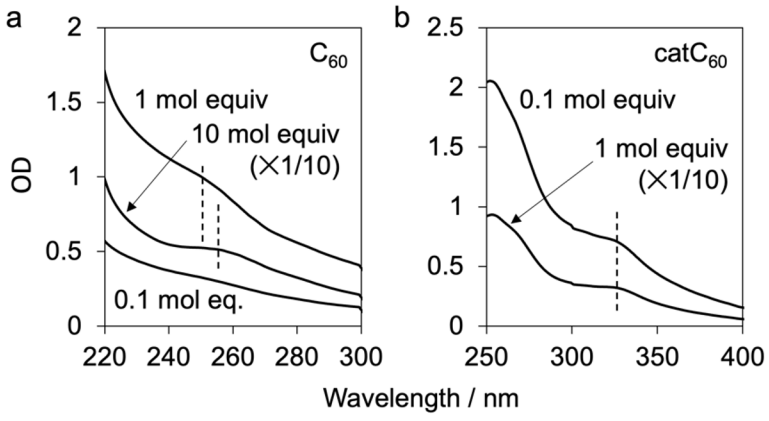

Figure 3: UV–vis absorption spectra of liposomes (1 mM phospholipid) with C_{60} (a) or a cationic derivative of C_{60} ($catC_{60}$) (b) added at various molar equivalents (mol equiv) to phospholipid. The equivalent of C_{60} added in C_{60}-loaded liposomes (C_{60}-lip) was 0.1, 1 and 10 mol equiv, and the equivalent of $catC_{60}$ added to $catC_{60}$-loaded liposomes ($catC_{60}$-lip) was 0.1 and 1 mol equiv. Spectra of 10 mol equiv of C_{60} in (a) and 1 mol equiv of $catC_{60}$ in (b) were measured after 10-fold dilution. The absorption peak positions for C_{60} and $catC_{60}$ are indicated with dotted lines. Liposome samples were dispersed in phosphate-buffered saline (PBS(–)).

$catC_{60}$, presumably by interacting in the liposome membrane. The incomplete quenching after the addition of PyBA at a concentration comparable to that of $catC_{60}$ may be attributed to the presence of unembedded PyBA in the dispersion. To this PyBA-embedded $catC_{60}$-lip system, methanol was added to completely destroy the liposome structures, resulting in the regain of the fluorescence intensity (Figure 4b). The results clearly demonstrate that PyBA interacts with $catC_{60}$ in the DMPC membrane near the surface, at least to some extent, indicating the potential of PyBA acting an anchor molecule to $catC_{60}$ in the liposome membrane. Nevertheless, further study is necessary to gain more insight into their location in the membrane.

The results above indicated the interaction of $catC_{60}$ with PyBA in the DMPC liposome membrane. We anticipated some effect of PyBA on the photoinduced generation of ROS by $catC_{60}$ due to such interaction within the liposome membrane. To investigate such effects, we employed an electron spin resonance (ESR) spin-trapping method to evaluate the generation of ROS by $catC_{60}$ in the absence or presence of PyBA. As spin trapping reagents for the singlet oxygen ($^1O_2$), hydroxyl radical (•OH) and superoxide radical anion (O_2•$^-$); 2,2,6,6,-tetramethyl-4-piperidone (4-oxo-TEMP), 3,4-dihydro-2,3-dimethyl-2*H*-pyrrole 1-oxide (DMPO), and 5-(diethoxyphosphoryl)-5-methyl-1-pyrrolidone-*N*-oxide (DEPMPO) were respectively used (schemes in Figure 5). Our previous study demonstrated that both $^1O_2$ and O_2•$^-$ were generated under irradiation of triad molecules in DMSO/H_2O [8].

Under irradiation by a blue LED (464–477 nm, 23 lm·W^{-1}), significant ESR signals corresponding to the $^1O_2$ adduct of 4-oxo-TEMP (4-oxo-TEMPO) were observed in the dispersion of $catC_{60}$-lip ([$catC_{60}$] = 5 μM) in PBS(–) showing an evidence of energy transfer reaction by the photoexcited $catC_{60}$ (Figure 5a(ii)). In the presence of electron donor (NADH) under photoirradiation, •OH generation was observed as a •OH adduct of DMPO (DMPO-OH, Figure 5b(ii)) revealing that electron transfer reaction was also occurring. Using DEPMPO as a spin trapping reagent, detection of O_2•$^-$ was tried and some radical adducts were detected, but without being clearly identified (Figure 5c(i), (ii)). The reason of the inability of O_2•$^-$ detection is not known at present. Upon addition of dimethyl sulfoxide (DMSO) to this system, an adduct of DEPMPO and •CH_3 (DEPMPO-CH_3), which was presumably generated from the reaction of •OH and DMSO, was clearly observed, further confirming the generation of •OH (Figure 5b(iii)). At the same time, unusually fast conversion of $O_2^{\bullet-}$ to •OH was also suggested in this system.

The results above suggest that $catC_{60}$-lip generated both types of ROS ($^1O_2$ and •OH) via energy transfer and electron transfer mechanisms. The present results are in line with previous studies of photoinduced ROS generation by C_{60} and its derivatives [17-19]. The most important: upon the addition of PyBA to $catC_{60}$-lip, the signal intensities of both types of ROS ($^1O_2$ and •OH) were decreased (Figure 5a(iii), b(iii), c(iv)). These results indicate that PyBA suppresses ROS generation by $catC_{60}$-lip in liposome environment, which would be advantageous for the nanoscale control of V_m by the triad molecules.

Conclusion

In summary, our findings indicate that PyBA can interact with $catC_{60}$ within DMPC liposomes and modestly inhibit the photoinduced generation of ROS by $catC_{60}$. These insights offer

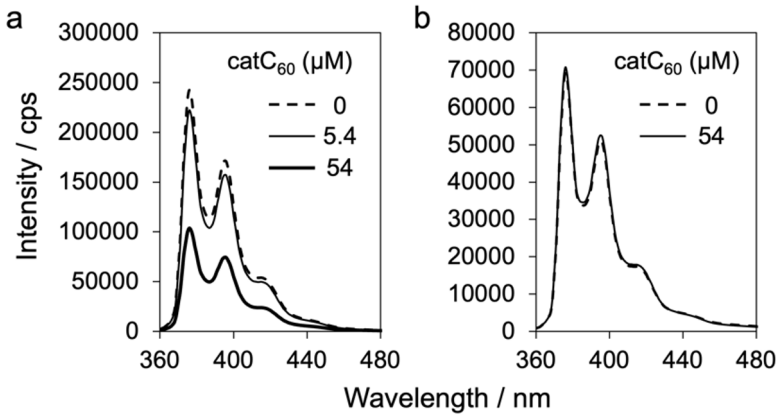

Figure 4: Fluorescence spectra of 1-pyrenebutyric acid (PyBA) in cationic derivative of C_{60} ($catC_{60}$)-loaded liposomes ($catC_{60}$-lip, 1 mM phospholipid) containing $catC_{60}$ at various concentrations. (a) Effect of $catC_{60}$ in liposomes on the fluorescence intensity of PyBA, with concentrations of $catC_{60}$ at 0, 5.4, 54 μM, and PyBA at 50 μM. (b) Fluorescence spectra of $catC_{60}$-lip with 0 and 54 μM $catC_{60}$, treated with 50 μM PyBA, after addition of methanol. Liposome samples were dispersed in phosphate-buffered saline (PBS(–)).

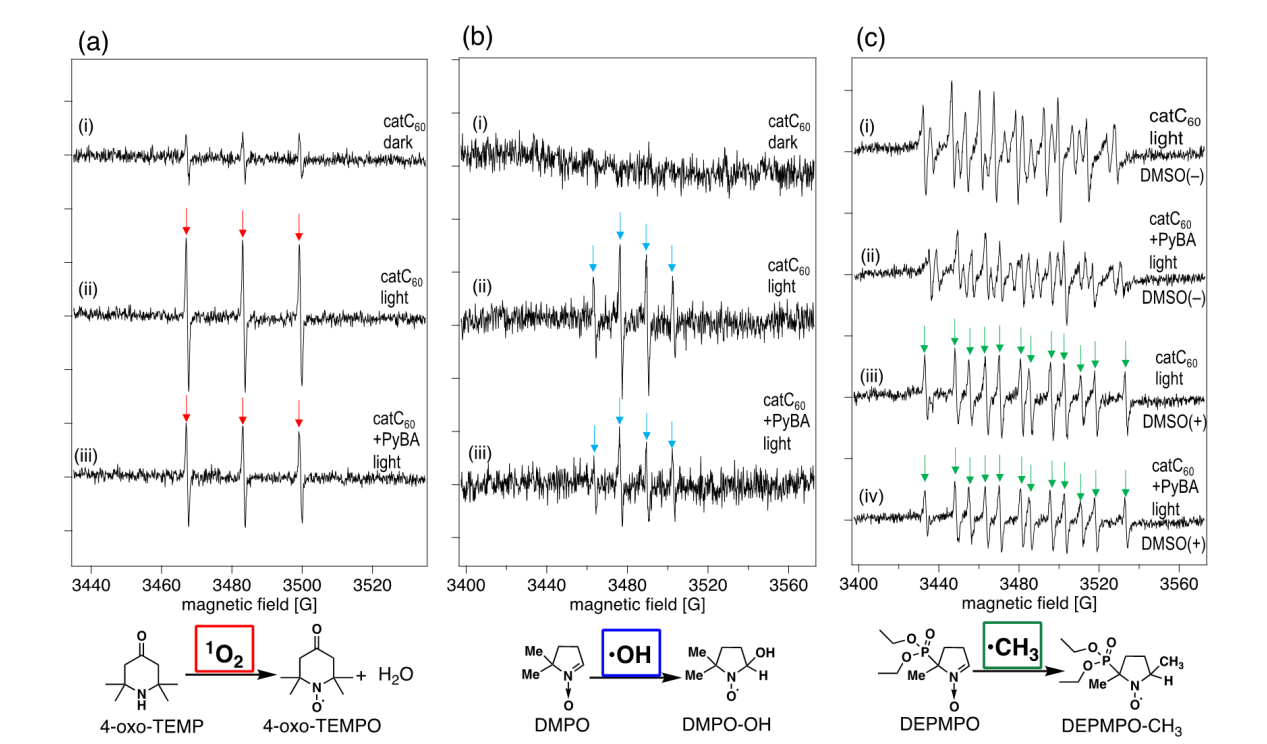

Figure 5: Photoinduced generation of reactive oxygen species (ROS) by cationic derivative of C_{60} ($catC_{60}$)-loaded liposomes ($catC_{60}$-lip) (5 μM $catC_{60}$) in the absence and presence of 1-pyrenebutyric acid (PyBA, 50 μM). (a) X-band electron spin resonance (ESR) spectra of 2,2,6,6,-tetramethyl-4-piperidone (4-oxo-TEMP) adduct with $^1O_2$ generated by $catC_{60}$ under irradiation by a blue LED. Experimental conditions: (i) $catC_{60}$ 5 μM and 4-oxo-TEMP 100 μM, in phosphate-buffered saline (PBS(–)) under dark conditions. (ii) $catC_{60}$ 5 μM and 4-oxo-TEMP 100 μM in PBS(–) under irradiation for 30 min by blue LED lamp. (iii) $catC_{60}$ 5 μM, PyBA 67 μM, and 4-oxo-TEMP 100 μM, in PBS(–) under irradiation for 30 min by blue LED lamp. (b) X-band ESR spectra of 3,4-dihydro-2,3-dimethyl-2*H*-pyrrole 1-oxide (DMPO) adduct with •OH generated by $catC_{60}$ under irradiation by a blue LED. Experimental conditions: (i) $catC_{60}$ 5 μM, β-nicotinamide adenine dinucleotide, reduced disodium salt hydrate (NADH) 8 mM, Fe(II)-diethylenetriaminepentaacetic acid (DETAPAC) 1 mM, and DMPO 100 mM in PBS(–) under irradiation for 30 min by blue LED lamp. (ii) $catC_{60}$ 5 μM, NADH 8 mM, Fe(II)-DETAPAC 1 mM, and DMPO 100 mM in PBS(–) under irradiation for 30 min by blue LED lamp. (iii) $catC_{60}$ 5 μM, PyBA 67 μM, NADH 8 mM, Fe(II)-DETAPAC 1 mM, and DMPO 100 mM in PBS(–) under irradiation for 30 min by blue LED lamp. (c) X-band ESR spectra of 5-(diethoxyphosphoryl)-5-methyl-1-pyrrolidone-*N*-oxide (DEPMPO) adduct with undefined radicals (i, ii) or •CH_3 (iii, iv) generated by $catC_{60}$ under irradiation by a blue LED. Experimental conditions: (i) $catC_{60}$ 5 μM, NADH 8 mM, DETAPAC 1 mM, and DEPMPO 100 mM in PBS(–) under irradiation for 30 min by blue LED lamp. (ii) $catC_{60}$ 5 μM, PyBA 67 μM, NADH 8 mM, DETAPAC 1 mM, and DEPMPO 100 mM in PBS(–) under irradiation for 30 min by blue LED lamp. (iii) $catC_{60}$ 5 μM, NADH 8 mM, DETAPAC 1 mM, and DEPMPO 100 mM in a 4-to-1 (v/v) mixture of PBS(–) and dimethyl sulfoxide (DMSO) under irradiation for 30 min by blue LED lamp. (iv) $catC_{60}$ 5 μM, PyBA 67 μM, NADH 8 mM, DETAPAC 1 mM, and DEPMPO 100 mM in a 4-to-1 (v/v) mixture of PBS(–) and DMSO under irradiation for 30 min by blue LED lamp. In the ESR spectra, signals corresponding to the adducts are indicated with red (4-oxo-TEMPO in a), blue (DMPO-OH in b), and green (DEPMPO-CH_3 in c) arrows.

valuable guidance for the photocontrol of the plasma membrane potential (V_m) using fullerene-containing triad molecules on a millisecond scale.

Experimental

Preparation of liposomes with $catC_{60}$ ($catC_{60}$-lip) or C_{60} (C_{60}-lip)

Liposomes were prepared using a thin-film hydration method. DMPC (NOF AMERICA Corporation, White Plains, NY, USA) was solubilized in ethanol (FUJIFILM Wako Pure Chemical Corporation, Osaka, Japan), and $catC_{60}$, which was synthesized according to a previous report [20], or C_{60} (NOF AMERICA Corporation, White Plains, NY, USA) was solubilized in a 1:4 (vol:vol) mixture of DMSO (Nacalai Tesque Inc., Kyoto, Japan) and toluene (FUJIFILM Wako Pure Chemical Corporation, Osaka, Japan). DMPC in ethanol and $catC_{60}$ or C_{60} in DMSO/toluene were mixed in molar ratios of 1:0, 1:0.1, 1:1, or 1:10, and the solvent was removed using a rotary evaporator (Rotavapor R-300, BÜCHI Labortechnik AG, Switzerland) at 40 °C to prepare the lipid films. The lipid films were then dried overnight in vacuo. Then, the films were hydrated with PBS(–) (137 mM NaCl, 2.68 mM KCl, 8.1 mM Na_2HPO_4, 1.47 mM KH_2PO_4) so that the theoretical value of DMPC concentration was 3 mg/mL, and the resulting suspension was sonicated at 30 °C until the lipid membrane had completely peeled off from the flask. To remove free $catC_{60}$ and C_{60}, the resulting suspension was centrifuged at 20,000*g* at room temperature for 10 min. The supernatant was collected and subjected to more than 20 extrusions using a Mini-Extruder equipped with a

100 nm-pore-size membrane (Croda International Plc. Avanti Polar Lipids, Inc.).

Differential scanning calorimetry (DSC)

DSC was performed using a MicroCal^{TM}PEAQ-DSC System (Malvern Panalytical, Ltd., Malvern, U.K.). Liposomal suspensions of DMPC with or without catC_{60} or C_{60} were dispersed in PBS(–) (1 mM DMPC). Measurements were performed following equilibration at 10 °C at a scan rate of 180 °C/h. Measurements were also performed after mixing of 50, 100 or 500 μM PyBA (Sigma-Aldrich, St. Louis, MI, USA) and DMPC liposomes without catC_{60} or C_{60} followed by dialysis of the mixture against 3 L PBS for 2 h to remove free PyBA. Data analysis, including calculation of the phase transition temperature, was performed using the MicroCal PEAQ-DSC Software.

UV–vis absorption measurement

UV–vis spectra of DMPC liposomes (1 mM DMPC) with or without catC_{60} or C_{60} were measured in PBS(–) using a UV-3600 Plus absorption spectrometer (Shimadzu Corporation, Kyoto, Japan).

Fluorescence measurement

DMPC liposomes containing 0, 5.4, or 54 μM catC_{60} were mixed with PyBA (final concentration of 50 μM) in PBS(–), and the mixture was dialysed against 3 L PBS for 2 h to remove free PyBA. Fluorescence spectra were measured using an RF-6000 spectrofluorometer (Shimadzu Corporation, Kyoto, Japan) (excitation at 341 nm, emission at 360–500 nm) to evaluate the interaction between catC_{60} and PyBA in DMPC membranes. Measurements were also performed after the addition of 10 times the volume of methanol to the liposome samples to liberate catC_{60} and PyBA from the membranes.

ESR measurements for photoinduced $^1O_2$ and $O_2^{\bullet-}$ generation

ESR spectra were recorded on a Bruker EMX, Continuous Wave X-Band EPR spectrometer (Bruker BioSpin GmbH, Rheinstetten, Germany). Suprasil® ESR tubes with a diameter of 4 mm, length of 250 mm and a wall thickness of 0.8 mm were used (SP Wilmad-LabGlass, New Jersey, US). 4-Oxo-TEMP was purchased from ABCR (Karlsruhe, Germany) and purified by sublimation prior to use. The 50 μL Blaubrand® intraMark capillaries were used in the EPR measurements (Brand GMBH, Wertheim, Germany). DEPMPO was bought from Enzo Life Sciences AG (Farmingdale, NY, USA). $FeSO_4$, DETAPAC and NADH was bought from Sigma-Aldrich (St. Louis, Missouri, USA). DMPO was bought from TCI (Tokyo Chemical Industry Co. Ltd., Tokyo, Japan). Irradiation was performed by blue LED light (464–477 nm, 23 lm·W^{-1}) from Lumiflex300 Pro RGB LED Stripes (LUMITRONIX LED-Technik GmbH, Hechingen, Germany) containing 120 LED lamps assembled in an aluminium cylindrical container with a diameter of 8.5 cm. ESR measurements conditions: microwave frequency 9.78 GHz, microwave power 10 mW, receiver gain 5.02×10^4, modulation amplitude 1.00 G, modulation frequency 100 kHz, 3 scan average, sweep time 83.89 s.

$^1O_2$ Generation: All measurements were performed in PBS(–). Ten μL of catC_{60} sample solution (25 μM), 10 μL of 4-oxo TEMP solution (500 mM) and 30 μL of PBS(–) were mixed in a 0.5 mL Eppendorf tube. For the measurement in the presence of PyBA, 10 μL of PyBA solution (335 μM) was added instead of 10 μM of PBS(–). The solution was subjected to O_2 bubbling for 30 seconds and then taken into 50 μL capillary and sealed. The solution was then irradiated with blue LED light for 30 minutes. The capillary was taken into the ESR tube for measurement at room temperature.

$^{\bullet}$OH Generation: All measurements were performed in PBS(–). Ten μL of catC_{60} sample solution (25 μM), 10 μL of Fe(II)-DETAPAC solution (5 mM), 10 μL of DMPO solution (500 mM), 10 μL of NADH (40 mM) and 10 μL PBS(–) were mixed in a 0.5 mL Eppendorf tube. For the measurement in the presence of PyBA, 10 μL of PyBA solution (335 μM) was added instead of 10 μL of PBS(–). The solution was subjected to O_2 bubbling for 30 seconds and then taken into 50 μL capillary and sealed. The solution was irradiated with blue LED light for 30 minutes. The capillary was taken into the ESR tube and ESR spectra were recorded at room temperature.

$O_2^{\bullet-}$ Generation: Measurements were performed in a mixture of DMSO and PBS(–) (1-to-4, v/v). Ten μL of catC_{60} sample solution (25 μM), 10 μL of DETAPAC solution (5 mM), 10 μL of DEPMPO solution (500 mM), 10 μL of NADH (40 mM) and 10 μL of PBS(–) were mixed in a 0.5 mL Eppendorf tube. For the measurement in the presence of PyBA, 10 μL of PyBA solution (335 μM) was added instead of 10 μL of PBS(–). The solution was subjected to O_2 bubbling for 30 seconds and then taken into 50 μL capillary and sealed. The solution was irradiated with blue LED light for 30 minutes. The capillary was taken into the ESR tube and ESR spectra were recorded at room temperature.

Acknowledgements

The authors thank Dr. Ebert from ETH Zurich for his support on ESR measurements.

Funding

This work was financially supported by JSPS KAKENHI Grant Number JP20H05842 [T.M.].

Author Contributions

Hayato Takagi: investigation; writing – original draft; writing – review & editing. Çetin Çelik: investigation; writing – review & editing. Ryosuke Fukuda: data curation; formal analysis; investigation. Qi Guo: investigation. Tomohiro Higashino: project administration; supervision; writing – review & editing. Hiroshi Imahori: project administration; supervision; writing – review & editing. Yoko Yamakoshi: formal analysis; methodology; project administration; supervision; validation; writing – review & editing. Tatsuya Murakami: conceptualization; data curation; formal analysis; funding acquisition; project administration; supervision; validation; writing – original draft; writing – review & editing.

ORCID® iDs

Hayato Takagi - https://orcid.org/0009-0009-3557-9730
Çetin Çelik - https://orcid.org/0000-0001-6132-8710
Ryosuke Fukuda - https://orcid.org/0000-0003-2509-3314
Tatsuya Murakami - https://orcid.org/0000-0001-5199-500X

Data Availability Statement

The data that supports the findings of this study is available from the corresponding author upon reasonable request.

References

1. Sariciftci, N. S.; Smilowitz, L.; Heeger, A. J.; Wudl, F. *Science* **1992,** *258,* 1474–1476. doi:10.1126/science.258.5087.1474
2. Yu, G.; Gao, J.; Hummelen, J. C.; Wudl, F.; Heeger, A. J. *Science* **1995,** *270,* 1789–1791. doi:10.1126/science.270.5243.1789
3. Imahori, H.; Kobori, Y.; Kaji, H. *Acc. Mater. Res.* **2021,** *2,* 501–514. doi:10.1021/accountsmr.1c00045
4. Cai, N.; Takano, Y.; Numata, T.; Inoue, R.; Mori, Y.; Murakami, T.; Imahori, H. *J. Phys. Chem. C* **2017,** *121,* 17457–17465. doi:10.1021/acs.jpcc.7b04466
5. Takano, Y.; Miyake, K.; Sobhanan, J.; Biju, V.; Tkachenko, N. V.; Imahori, H. *Chem. Commun.* **2020,** *56,* 12562–12565. doi:10.1039/d0cc05326k
6. Numata, T.; Fukuda, R.; Hirano, M.; Yamaguchi, K.; Sato-Numata, K.; Imahori, H.; Murakami, T. *Cell. Physiol. Biochem.* **2020,** *54,* 899–916. doi:10.33594/000000277
7. Imahori, H.; Tamaki, K.; Guldi, D. M.; Luo, C.; Fujitsuka, M.; Ito, O.; Sakata, Y.; Fukuzumi, S. *J. Am. Chem. Soc.* **2001,** *123,* 2607–2617. doi:10.1021/ja003346i
8. Takano, Y.; Numata, T.; Fujishima, K.; Miyake, K.; Nakao, K.; Grove, W. D.; Inoue, R.; Kengaku, M.; Sakaki, S.; Mori, Y.; Murakami, T.; Imahori, H. *Chem. Sci.* **2016,** *7,* 3331–3337. doi:10.1039/c5sc04135j
9. Qiao, R.; Roberts, A. P.; Mount, A. S.; Klaine, S. J.; Ke, P. C. *Nano Lett.* **2007,** *7,* 614–619. doi:10.1021/nl062515f
10. Ikeda, A.; Kiguchi, K.; Shigematsu, T.; Nobusawa, K.; Kikuchi, J.-i.; Akiyama, M. *Chem. Commun.* **2011,** *47,* 12095–12097. doi:10.1039/c1cc14650e
11. Jablonski, A. E.; Kawakami, T.; Ting, A. Y.; Payne, C. K. *J. Phys. Chem. Lett.* **2010,** *1,* 1312–1315. doi:10.1021/jz100248c
12. Takeuchi, T.; Kosuge, M.; Tadokoro, A.; Sugiura, Y.; Nishi, M.; Kawata, M.; Sakai, N.; Matile, S.; Futaki, S. *ACS Chem. Biol.* **2006,** *1,* 299–303. doi:10.1021/cb600127m
13. Bangham, A. D.; Standish, M. M.; Watkins, J. C. *J. Mol. Biol.* **1965,** *13,* 238–252. doi:10.1016/s0022-2836(65)80093-6
14. Ikeda, A.; Mae, T.; Ueda, M.; Sugikawa, K.; Shigeto, H.; Funabashi, H.; Kuroda, A.; Akiyama, M. *Chem. Commun.* **2017,** *53,* 2966–2969. doi:10.1039/c7cc00302a
15. Numata, T.; Murakami, T.; Kawashima, F.; Morone, N.; Heuser, J. E.; Takano, Y.; Ohkubo, K.; Fukuzumi, S.; Mori, Y.; Imahori, H. *J. Am. Chem. Soc.* **2012,** *134,* 6092–6095. doi:10.1021/ja3007275
16. Sluch, M. I.; Samuel, I. D. W.; Petty, M. C. *Chem. Phys. Lett.* **1997,** *280,* 315–320. doi:10.1016/s0009-2614(97)01159-7
17. Yamakoshi, Y.; Umezawa, N.; Ryu, A.; Arakane, K.; Miyata, N.; Goda, Y.; Masumizu, T.; Nagano, T. *J. Am. Chem. Soc.* **2003,** *125,* 12803–12809. doi:10.1021/ja0355574
18. Serda, M.; Szewczyk, G.; Krzysztyńska-Kuleta, O.; Korzuch, J.; Dulski, M.; Musioł, R.; Sarna, T. *ACS Biomater. Sci. Eng.* **2020,** *6,* 5930–5940. doi:10.1021/acsbiomaterials.0c00932
19. Liosi, K.; Stasyuk, A. J.; Masero, F.; Voityuk, A. A.; Nauser, T.; Mougel, V.; Solà, M.; Yamakoshi, Y. *JACS Au* **2021,** *1,* 1601–1611. doi:10.1021/jacsau.1c00239
20. Guo, Q.; Ghalei, B.; Qin, D.; Mizutani, D.; Joko, I.; Al-Aziz, H.; Higashino, T.; Ito, M. M.; Imahori, H.; Sivaniah, E. *Chem. Commun.* **2023,** *59,* 10012–10015. doi:10.1039/d3cc02175k

License and Terms